

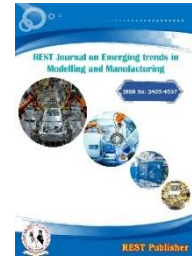
## REST Journal on Emerging trends in Modelling and Manufacturing

Vol: 11(1), March 2025

REST Publisher; ISSN: 2455-4537 (Online)

Website: <https://restpublisher.com/journals/jemm/>

DOI: <https://doi.org/10.46632/jemm/11/1/5>



# Smart Transformer based Battery Energy Storage Systems Using ANFIS with enhanced Energy Efficiency and SOC Management

\*B.N. Prasad, C. Prudhvi, N. Chandana, M. Siva Mohan, K. R. Rajendra Prasad, S. Aslam Basha

Annamacharya Institute of Technology & Sciences (Autonomous) Kadapa, Andhra Pradesh, India.

\*Corresponding Author Email: [bingimalla.n.prasad@gmail.com](mailto:bingimalla.n.prasad@gmail.com)

**Abstract:** A smart transformer (ST), which is a power-electronic-based transformer with control and communication functionalities, can be the optimal solution for integrating a battery energy storage system (BESS) in an electric distribution system. This paper investigates the performance of a ST-based BESS in comparison to a conventional BESS, focusing on energy efficiency during charging and discharging processes. Results show that the ST-based BESS operation outperforms the conventional system, particularly in terms of energy efficiency. Additionally, by appropriately sizing the BESS to meet peak load demands, the power rating of ST converters can be minimized. The ST-based BESS also demonstrates enhanced fault ride-through capabilities compared to traditional systems. To ensure the proper functioning of the ST-based BESS, effective state of charge (SOC) management is critical, especially when the ST converter operates at its maximum active power rating. In this context, an Adaptive Neuro-Fuzzy Inference System (ANFIS) is utilized for optimal SOC management, ensuring that the system efficiently meets peak load demand while avoiding over-discharge or over-charge. Both simulation and experimental results validate the developed ANFIS-based SOC management approach, confirming its effectiveness in enhancing the system's performance.

## 1. INTRODUCTION

The global demand for clean and sustainable energy sources is rising rapidly, primarily due to the growing concern over environmental impacts caused by traditional fossil fuels. As renewable energy generation, especially solar and wind power, continues to increase, the intermittency and variability of these resources pose significant challenges to grid stability and reliability. These challenges have spurred the development of advanced energy systems capable of integrating renewable energy sources into the existing electrical grid while maintaining a high level of reliability and efficiency. Among the various solutions, Battery Energy Storage Systems (BESS) have emerged as a promising option for addressing these challenges by providing energy storage, regulation of voltage, and support for grid stability. However, to ensure that BESS can effectively contribute to grid reliability and efficiency, integrating advanced technologies like Smart Transformers (ST) can further enhance their functionality and performance.

**Smart Transformers (ST) and Battery Energy Storage Systems (BESS):** A Smart Transformer (ST) is a power-electronic-based transformer that integrates control and communication functionalities into the conventional transformer design. Unlike traditional transformers, which rely primarily on magnetic induction, STs employ power electronic devices such as converters, controllers, and sensors to regulate voltage, control power flow, and facilitate communication between the transformer and the grid. STs offer several advantages over traditional transformers, including increased efficiency, flexibility, and fault tolerance. The integration of STs into electric distribution systems provides an effective solution for improving the operation of renewable energy-based grids, particularly in conjunction with Battery Energy Storage Systems (BESS). Battery Energy Storage Systems (BESS) have become critical components for enhancing the performance and reliability of electrical grids. A BESS stores electrical energy in the form of chemical energy in batteries and releases it when needed. The primary function of BESS is to balance the supply and demand of electricity, smooth out fluctuations in renewable energy generation, and support grid stability. BESS can store excess electricity generated during periods of high renewable energy production and discharge this stored energy during periods of high demand or low generation, thus reducing reliance on fossil-fuel-based generation and ensuring grid reliability. However, integrating

BESS into the grid presents several challenges, particularly related to the energy efficiency during charging and discharging processes, as well as the ability to handle fault conditions. Traditional BESS systems often suffer from energy losses due to their reliance on conventional transformers and lack the flexibility to dynamically adjust to grid conditions. The integration of STs with BESS has the potential to address these limitations by providing more efficient and adaptable control over the charging and discharging processes, as well as enhancing the overall performance of the system.

**Energy Efficiency and Charging/Discharging Process:** One of the key considerations when evaluating the performance of a BESS is its energy efficiency during charging and discharging. Energy losses can occur during these processes due to various factors, including the inefficiencies of the power electronics, transformer losses, and the characteristics of the battery itself. In traditional systems, the energy efficiency during the charging and discharging processes is often lower due to the use of conventional transformers and simple control strategies. As a result, a significant portion of the energy that is supposed to be stored or discharged may be lost, reducing the overall efficiency of the system. The introduction of Smart Transformers (ST) into the system can significantly improve the energy efficiency during the charging and discharging processes. STs incorporate advanced power electronics and control mechanisms that optimize the flow of electricity between the grid, the BESS, and the load. By employing high-efficiency converters, STs can reduce energy losses during the power conversion stages, resulting in higher overall system efficiency. Additionally, the intelligent control features of STs enable more precise regulation of power flow, minimizing energy losses and improving the charging and discharging efficiency of the BESS.

**Sizing and Power Rating Optimization:** The effective sizing of a Battery Energy Storage System (BESS) is crucial for ensuring that it can meet peak load demands without over-sizing or under-sizing the system. An oversized BESS may result in unnecessary capital costs and inefficiencies, while an undersized BESS may fail to provide adequate support during peak load conditions. One of the advantages of integrating STs into the BESS configuration is that the power rating of the ST converters can be optimized to match the required load demands. By properly sizing the BESS to meet peak load requirements, the power rating of the ST converters can be minimized, which not only reduces the cost of the system but also enhances its efficiency.

In a conventional BESS system, the power rating of the converter is typically fixed, and it may not be fully utilized during certain periods. However, with a Smart Transformer-based BESS, the converter power rating can be dynamically adjusted based on the system's load demand and the state of charge (SOC) of the battery. This dynamic adjustment allows for better utilization of the converter's capacity, resulting in a more efficient operation of the system and reduced energy losses. Additionally, STs can adapt to changing grid conditions and optimize the operation of the BESS based on real-time data, further improving system performance.

**Fault Ride-Through Capabilities:** Grid faults, such as voltage sags, short circuits, or sudden changes in load, can pose significant challenges to the operation of energy storage systems. Conventional BESS systems may struggle to handle such disturbances, leading to instability and potential damage to the system. One of the key advantages of integrating Smart Transformers with BESS is their enhanced fault ride-through capabilities. Smart Transformers are equipped with advanced control and protection mechanisms that allow them to respond dynamically to grid faults and ensure the stability of the BESS during such events.

In the event of a fault, STs can quickly detect and isolate the faulted section, preventing the propagation of disturbances throughout the system. Moreover, the ST-based BESS can continue to operate even under fault conditions, ensuring that the energy storage system remains available to support the grid. This enhanced fault tolerance is particularly important for ensuring the reliability of the energy storage system in critical applications, such as supporting renewable energy integration or providing backup power during grid outages.

**State of Charge (SOC) Management:** Effective State of Charge (SOC) management is essential for optimizing the operation of a Battery Energy Storage System (BESS). SOC refers to the percentage of energy remaining in the battery relative to its maximum capacity. Maintaining an optimal SOC is crucial for ensuring the efficient operation of the BESS, preventing over-discharge or over-charge, and prolonging the life of the battery. The SOC management of a BESS can be challenging, especially when the system operates at or near its maximum power rating. In such cases, improper SOC management can lead to excessive cycling of the battery, reducing its lifespan and decreasing the overall system efficiency. To address this challenge, advanced control strategies are required to monitor and manage the SOC of the BESS in real time. An effective approach for SOC management is the use of Adaptive Neuro-Fuzzy Inference Systems (ANFIS). ANFIS is a hybrid artificial intelligence system that combines the strengths of neural networks and fuzzy logic to model and control complex, nonlinear systems. By using ANFIS, it is possible to develop a control algorithm that optimizes the SOC of the BESS based on real-time data, ensuring that the system efficiently meets peak load demands while avoiding over-discharge or over-charge. The ANFIS-based SOC management approach can also adapt to changing grid conditions, further improving the performance of the BESS.

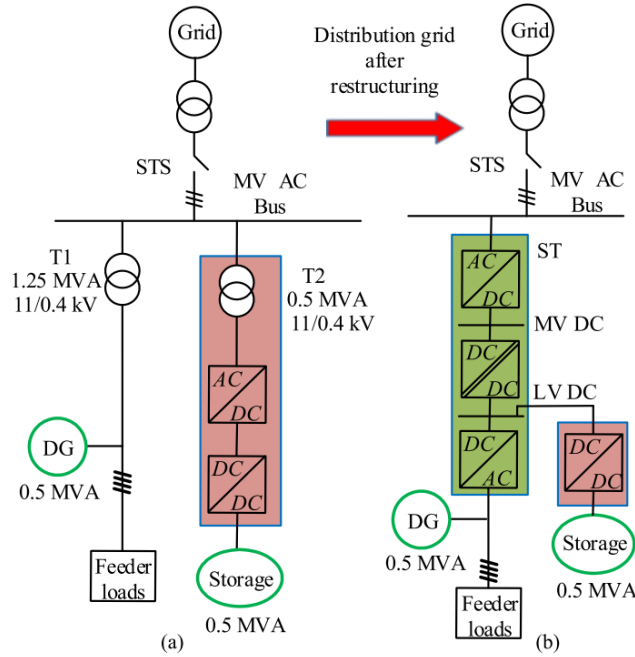


FIGURE 1. Single-line diagram. (a) Conventional distribution electric grid. (b) Restructured distribution electric grid with transformer T1 is replaced by an ST, and the BESS is integrated into the LV dc-link of the ST

## 2. DESCRIPTION OF THE SYSTEM CONFIGURATION

**Conventional System Configuration:** A single-line diagram of the considered conventional power system is shown in Fig. 1(a) [21], [22]. The loads are connected to the MV ac bus through a transformer T1. An inverter-based DG system is connected to the line. The BESS is connected to the MV bus to store the energy generated through the DG as well as to supply loads during contingency. The BESS consists of a CPT T2, an ac–dc converter, and a dc–dc converter. The BESS is rated for 0.5 MVA with a battery bank having a capacity of 0.5 MWh. The rated voltage of the battery bank is 620 V with 10% variations from the rated value.

TABLE 1. Conventional System Parameters

	Load power	Equipment rating
Line	Active = 0.7 MW Reactive = 0.6 MVar Apparent = 0.92 MVA	Transformer T1 = 1.25 MVA
BESS		dc–dc converter = 0.5 MVA ac–dc converter = 0.5 MVA Transformer T2 = 0.5 MVA

TABLE 2. Proposed St-Based Bess: Power Converter Rating

Power converter	Power converter rating
ST inverter	1.25 MVA
ST dc–dc converter	0.575 MVA
ST rectifier	0.65 MVA
BESS dc–dc converter	0.5 MVA

**ST-Based BESS Configuration:** As shown in Fig. 1(b), a three-power-conversion-stage ST replaces the line CPT T1. The ac–dc stage of the ST, also called the ST rectifier, controls the MV grid side currents to ensure that the appropriate active power is exchanged while regulating the MV dc-link voltage around a reference voltage. The second stage is an isolated dc–dc converter, which converts MV dc to LV dc, provides an isolation between the MV and LV dc links, and regulates the LV dc link at a reference voltage. The third stage converter, the dc–ac converter or the ST inverter, maintains a constant balanced sinusoidal ac voltage at the LV side and supports the loads of line. The DG configuration remains the same in the proposed scheme. The LV dc link of the ST is utilized to integrate the BESS to the electric grid. A dc–dc converter is used to charge/discharge the battery bank. The MV dc and LV dc links of the ST are maintained at voltages of 30 and 1.2 kV, respectively. The battery specification remains the same as the conventional system.

### Sizing Of Different Power Converters

The parameters of the conventional system configuration are given in Table I. In the proposed configuration, parameters given in Table II, both CPTs T1 and T2 are replaced by an ST. Also, the ac–dc converter of the BESS is eliminated. With the proper consideration of load demand and BESS capacity, an appropriate reduction in the sizing of the different power converters is also achieved.

**Battery Bank and BESS :** DC-DC Converter Under fully charged conditions, the BESS can supply 125-kW power continuously for 4 h. An averaged load profile, shown in Fig. 2, reveals that the average load demand is much lower than the rated power demand at most of the time of the day. The battery bank achieves its maximum SOC during day time by absorbing the DG power and supports the load during peak evening hours. Considering the SOC of the battery bank and the capability of continuously supplying the power, evening 4-h period is considered the peak load demand in this paper. The dc–dc converter is rated at 0.5 MVA to support the rated charging and discharging rate.

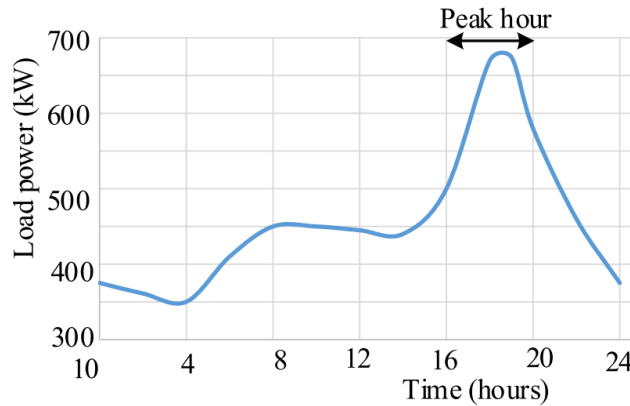


FIGURE 2. Averaged load profile in a typical residential feeder [23]

**Sizing of the ST Inverter :** In the worst-case scenario when the DG output is zero, the inverter will completely supply the rated active, reactive, and harmonic powers of load. In this regard, the ST inverter power rating,  $S_{inv-rated}$ , is given as

$$S_{inv-rated} = \sqrt{P_{l-rated}^2 + Q_{l-rated}^2 + H_{l-rated}^2}$$

where  $P_{l-rated}$ ,  $Q_{l-rated}$ , and  $H_{l-rated}$  are rated active, reactive, and harmonic load powers, respectively. The load demand is kept the same in the proposed configuration, and therefore, the ST inverter of 1.25 MVA is selected.

**Sizing of the ST DC–DC Converter:** As already explained, the worst-case scenario is encountered when the DG power is zero during the rated load demand. In that case, the load power is shared by the BESS and the grid. During peak hours, let  $P_{bess-peak}$  be the power that the BESS supplies continuously. Therefore, the isolated dc–dc converter rating,  $P_{dc-dc-rated}$ , is given as

$$P_{dc-dc-rated} = P_{l-rated} - P_{bess-peak}$$

Here,  $P_{l-rated}$  is 0.7 MW and  $P_{bess-peak}$  is 0.125 MW. This requires the dc–dc converter of the ST to be rated for 0.575 MW.

**Sizing of the ST Rectifier :** The ST isolated dc–dc converter and the rectifier transfer the same active power at any given time, and therefore, the rectifier active power rating ( $P_{rec-rated}$ ) is the same as that of the isolated converter rating. However, the ST rectifier must also have a sufficient capability to support the reactive power similar to the conventional BESS. Let  $Q_{rec-rated}$  be the ST-rectifier -rated reactive power compensation during the peak load conditions. Therefore, the ST rectifier apparent power rating will be

$$S_{rec-rated} = \sqrt{Q_{rec-rated}^2 + P_{dc-dc-rated}^2}$$

We consider that the ST has the capability to supply 0.3 MVar into the MV grid when it exchanges rated active power with the grid. Therefore, the ST rectifier is rated for 0.65 MVA.

### Power Flow In The Proposed St-Based Bess

Power flow for different operating modes is explained as follows.

**Normal Operation (BESS Charging Done by the DG) :** The load reactive and harmonic power is always supplied by the ST inverter. The active power flow depends upon the degree of availability of the DG and the load demand. In case I, as shown in Fig. 3(a), DG power ( $P_{DG}$ ) is more than the active load power ( $P_L$ ), and the battery bank is not fully charged. Therefore, rest of the power will be used for charging the battery bank. The ST rectifier and the dc–dc converter will not exchange power in this case (except the converter loss component). Once the battery bank is fully charged, this active power is injected into the MV grid through the rectifier and the dc–dc converter of the ST. The BESS converter draws power in this case. The corresponding power flow, as case II, is shown in Fig. 3(b). Fig. 3(c) shows power flow during case III when the DG power is not sufficient to meet the load power demand. In this situation, the load power deficit is supplied by the MV grid through the ST. As soon as the ST converters process rated power, the BESS is activated to supply the remaining power, as shown in Fig. 3(d).

**Emergency Operation (BESS Charging Done by the MV Grid) :** The DG remains out of operation for a long time either due to maintenance or due to weather conditions, and the BESS is charged from the MV grid. The BESS charging is realized, as shown in Fig. 3(e), when the load demand is lower than the ST power converter rating. Moreover, this charging scheme of the BESS is only an emergency arrangement.

### Efficiency Comparison

The battery bank is charged from the DG power in both configurations, as shown in Fig. 4. In the conventional scheme, the DG power is processed through feeder transformer T1, BESS transformer T2, the BESS ac–dc converter, and the BESS dc–dc converter during the charging and vice versa. Consider  $\eta_{T1}$ ,  $\eta_{T2}$ ,  $\eta_{ac/dc}^{bess}$ , and  $\eta_{dc/dc}^{bess}$  as the efficiency of transformer T1, transformer T2, the BESS ac–dc converter, and the BESS dc–dc converter, respectively. In this case, the overall efficiency of the devices during charging is given as

$$\eta_{con-charging} = \eta_{T1} \eta_{T2} \eta_{ac/dc}^{bess} \eta_{dc/dc}^{bess}$$

In the ST-based BESS, the charging and discharging process is shown in Fig. 4(b). The dc–ac converter of the ST (efficiency of  $\eta_{ST ac/dc}$ ) and the dc–dc converter of the BESS is involved in this process. In this case, the overall efficiency of the devices during charging is given as

$$\eta_{pro-charging} = \eta_{ac/dc}^{ST} \eta_{dc/dc}^{bess}$$

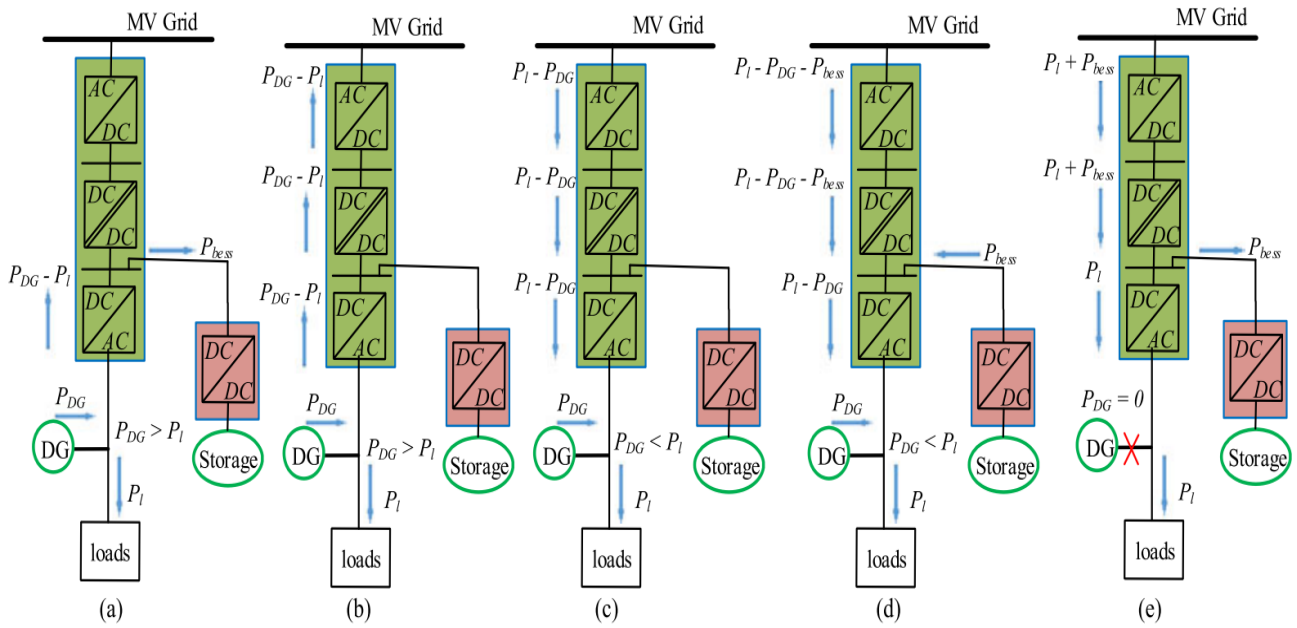


FIGURE 3. Power flow diagram in the proposed system

- (a) Case I:  $P_{DG} > P_L$  : The battery bank is not fully charged, and the surplus power is fed to charge battery.
- (b) Case II:  $P_{DG} > P_L$  : The battery bank is fully charged, and surplus power is injected into the MV grid.
- (c) Case III:  $P_{DG} < P_L$  : The MV grid supplies rest of the power through the ST.
- (d) Case IV:  $P_{DG} < P_L$  : The ST takes rated power from the MV grid and the rest of the load demand is met by the BESS.
- (e) Case V (DG is out of service for long time): The BESS is charged from the MV grid during nonpeak hours.

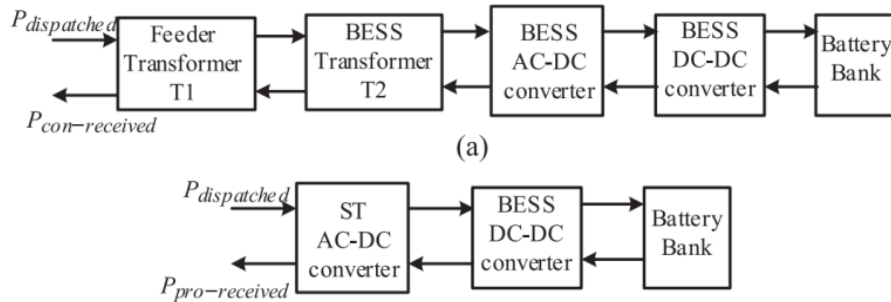


FIGURE 4. Power flow during charging and discharging. (a) Conventional BESS. (b) ST-based BESS

The comparison of the energy efficiency curve in the conventional and proposed configurations for charging the battery bank. The curves show the efficiency at different loading of different devices. The different topologies chosen are the cascaded H bridge for the ST MV converter, the ST dc–dc converter based on SiC devices [24], the standard three-phase inverter for the ST LV inverter, and the half-bridge converter for the battery charger. The efficiency curves are evaluated considering the manufacturer’s data and the scientific literature [25]–[27]. If the power of the prototype is lower than the target one, parallel connection is assumed, so the efficiency curves are simply upscaled to match the rated power. This choice may underestimate the efficiency, since higher power converters normally present higher values; however, it is coherent with a modular approach and enables a fault-tolerant system [28]. Due to the absence of many realization for isolated MV/LV dc–dc converters, the data from the literature are analyzed. It is evidenced that the efficiencies of such systems with Si devices are not competitive [29], and this is mainly because insulated-gate bipolar transistors are optimized for hard-switching operation, while the dc–dc converter is designed to operate in soft switching. Only for this stage, SiC devices are used, such as in [24], where a Si-based solid-state transformer was improved by adding a SiC-based dc–dc stage. In a previous experimental work, very high efficiencies could be obtained with SiC-based modular isolated dc–dc converters [30]. Moreover, similar to the efficiency of a PV converter, the average charging efficiency of the BESS can also be computed. A typical curve showing the voltage, current, and the charge capacity of a battery is shown in Fig. 6. Considering the different charging stages and time intervals, in a similar fashion to what happens for PV systems with the European or California efficiency, a possibility to compute the average efficiency is described as follows:

$$\eta_{\text{charge-avg}} = (0.7 \eta_{\text{max}}) + (0.2 \eta_{20}) + (0.1 \eta_{10})$$

Taking the values of efficiency at different loading conditions from Fig. 5, the average charging efficiency for the ST-based BESS is 95.81%. However, the CPT-based BESS has an average efficiency of 92.6%. In [31], it was measured that the battery discharge process can be 1% less efficient as compared to the charging process. Therefore, the proposed ST-based scheme will have a round trip efficiency of 90.8%, as compared to 84.8% in the conventional BESS system. Therefore, the proposed ST-based BESS is significantly efficient in comparison to the CPT-based BESS during charging as well as discharging. Consequently, it results in lower overall loss, better utilization of the DG power, and more savings on electricity bills.

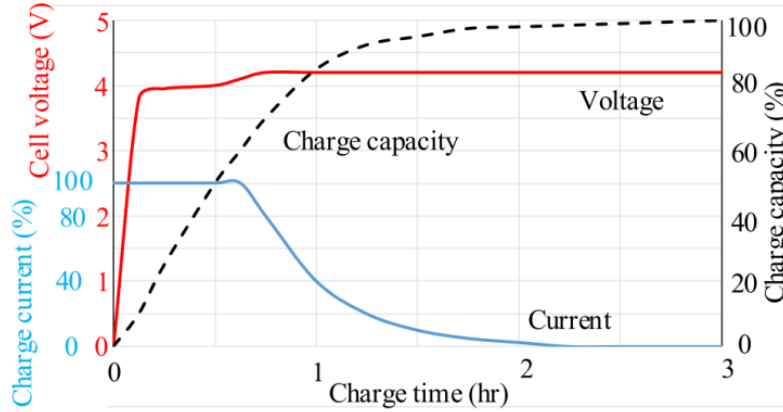


FIGURE 5. Typical curve for voltage, current, and SOC during charging of the battery (at 1 C)

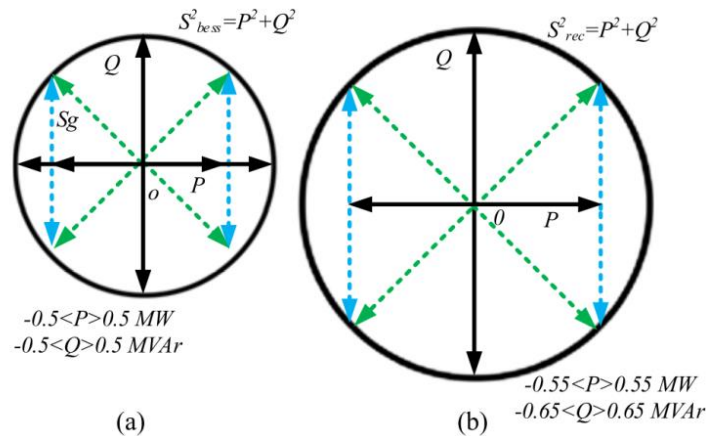


FIGURE 6. Reactive power support capability curve. (a) Conventional BESS configuration. (b) ST-based BESS configuration

**Reactive Power Support Capability :** In addition to the active power support, the BESS in the conventional configuration also provides ancillary services in the MV distribution grid by appropriate injection of the reactive power. The ancillary services are realized by effective control of the active and reactive powers of the grid-side converter, which is limited by their fixed apparent power rating. Let S, P, and Q be the apparent power, the active power, and the reactive power exchanged by the power converter with the grid, respectively, and these are related as follows:

$$S = \sqrt{Q^2 + P^2}$$

The capability curves for the conventional and proposed structures are shown in Fig. 7(a) and (b), respectively. It can be seen that in the ST-based BESS, a significantly large amount of reactive power can be injected into the grid compared to the conventional configuration. When the BESS charges/discharges at rated power, the proposed scheme has enough reactive power compensation capability as compared to negligible compensation capability in the conventional scheme

**Reliability Of The Proposed System :** Conventional transformers have nowadays a very high reliability, which is still higher than a power-electronics-based solution. However, research on improving the reliability of actual solutions [10] as well as in improving the materials has already shown pothessibility of improvement. Moreover, the implementation of fault-tolerant and repairable systems [32] is expected to further reduce the gap between the reliability of the CPT and the ST. If only the BESS is considered, then the proposed structure for charging/discharging uses a lower number of

components as compared to the conventional BESS (a conventional BESS is realized using an ac–dc converter, a dc–dc converter, and a CPT, whereas the proposed scheme uses an ac–dc converter and a dc–dc converter). Considering that the CPT is highly reliable and both the schemes use equal number of power converters, the reliability of the BESS configuration can be assumed to be the same. However, when the proposed overall system is considered, more number of power converters are employed in comparison to the conventional CPT-based BESS, and therefore, presently, the reliability of the ST-based system will be lower than the CPT-based system.

### 3. OPERATION AND CONTROL

#### Control of the ST Rectifier

The rectifier draws active power requested from the MV grid to support the loads and also maintains MV dc-link capacitor voltage at a constant value. Moreover, it injects reactive power to provide ancillary services if needed. In this paper, reference currents of the rectifier are generated using instantaneous symmetrical component theory (ISCT) [33]. With the ISCT, the rectifier reference currents are given as follows:

$$i_{rec-a}^* = \frac{v_{ta1}^+ + \frac{\tan\theta}{\sqrt{3}}(v_{tb}^+ - v_{tc}^+)}{(v_{ta1}^+)^2 + (v_{tb1}^+)^2 + (v_{tc1}^+)^2} (P_{rec}^* + P_{loss})$$

$$i_{rec-b}^* = \frac{v_{tb1}^+ + \frac{\tan\theta}{\sqrt{3}}(v_{tc}^+ - v_{ta}^+)}{(v_{ta1}^+)^2 + (v_{tb1}^+)^2 + (v_{tc1}^+)^2} (P_{rec}^* + P_{loss})$$

$$i_{rec-c}^* = \frac{v_{tc1}^+ + \frac{\tan\theta}{\sqrt{3}}(v_{ta}^+ - v_{tb}^+)}{(v_{ta1}^+)^2 + (v_{tb1}^+)^2 + (v_{tc1}^+)^2} (P_{rec}^* + P_{loss})$$

where  $v_{+ta1}$ ,  $v_{+tb1}$ , and  $v_{+tc1}$  are fundamental positive-sequence point of common coupling (PCC) voltages in three phases at the MV side. The angle  $\theta$  is a power factor angle responsible for reactive power injection.  $\theta$  is the angle between active and reactive powers exchanged by the ST with the MV grid. For a reactive power demand of  $Q_{rec}^*$ , the power factor angle  $\theta$  will be equal to  $\tan^{-1} \frac{Q_{rec}^*}{P_{rec}^* + P_{loss}}$ . Moreover, setting of  $\theta = 0$  will ensure that the reactive power is not exchanged from the MV grid. The power  $P_{loss}$  is the total power losses in the ST, and it helps in maintaining the MV dc-link voltage at a reference voltage. It is computed using a proportional–integral (PI) controller as follows:

$$P_{loss} = K_{p-mv} e_{dc-mv} + K_{i-mv} \int e_{dc-mv} dt$$

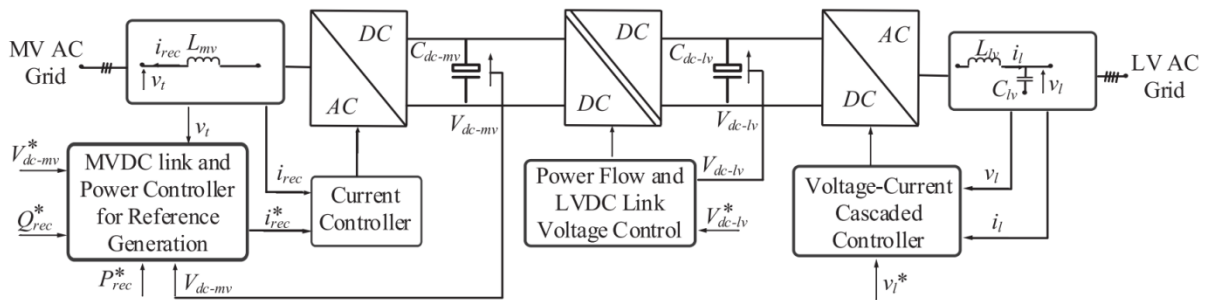
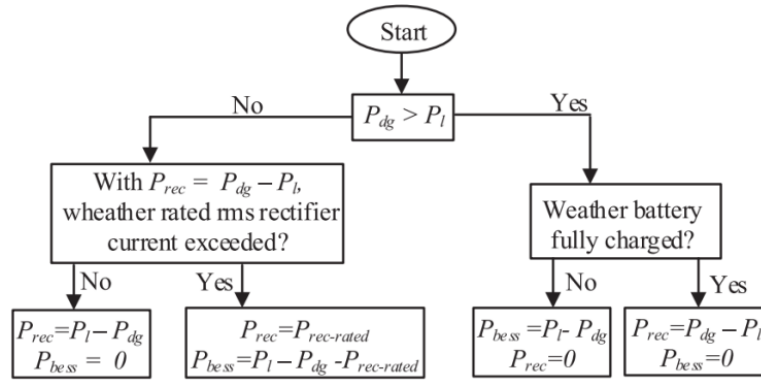


FIGURE 7. ST control block diagram





**FIGURE 8.** Flowchart to select ST rectifier and BESS power

where  $K_p$ -mv,  $K_i$ -mv, and  $e_{dc}$ -mv =  $V_{dc}$ -mv -  $V_{dc}$ -mv are the proportional gain, the integral gain, and the voltage error of the PI controller, respectively. The parameters of the PI controller are tuned with the symmetrical optimum criterion [1]. The overall control block diagram of the ST is given in Fig. 8. In (8), the power  $P^*_{rec}$  is rectifier power requested from the grid. It will be different for different operating conditions, as shown in Fig. 9 and also explained as follows.

Case I: If DG power is greater than load power and the battery is not fully charged, then rest of the power is used to charge the BESS. In this case, we have

$$P^*_{rec} = 0.$$

Case II: If DG power is greater than load power and the battery is fully charged, then rest of the power is send to the MV grid, i.e.,

$$P^*_{rec} = -(P_{DG} - P_l)$$

Case III: If DG power is lower than the load power requirement, then rest of the power is taken from the MV grid, provided that the rectifier does not reach its rated value, i.e.,

$$P^*_{rec} = P_{DG} - P_l$$

Case IV: Once the rectifier power reaches its rated value, i.e.,  $P^*_{rec} = P_{rec-rated}$ , then the deficit of the power is supplied by the BESS. This situation arises during peak load periods or during grid faults.

### Control of the ST DC-DC Converter

This converter maintains the power balance between two dc links and regulates the LV dc-link voltage at a constant value. The regulation of the LV dc link is achieved using a PI controller. The actual and reference LV dc-link voltages are compared to each other, and the error is passed through a PI controller having output as an angle  $\phi$

$$\phi = K_{p-lv} e_{dc-lv} + K_{i-lv} \int e_{dc-lv} dt$$

where  $K_p$ -lv,  $K_i$ -lv, and  $e_{dc}$ -lv =  $V_{dc}$ -lv -  $V_{dc}$ -lv are the proportional gain, the integral gain, and the voltage error of the PI controller, respectively.  $\phi$  is the angle between the pulsed voltages of two sides of the converter and ensures that the power flow is maintained between two dc links. The power transferred from one side of this converter to the other side is given as follows [16]:

$$P_{dc-dc} = \frac{V_{dc-lv} V_{dc-mv}}{2\pi f_{sw} L_{dc-dc}} \phi \left( 1 - \frac{|\phi|}{\pi} \right)$$

where  $L_{dc-dc}$  is the leakage impedance of the high-frequency transformer, and  $f_{sw}$  is the switching frequency of the converter. The converter power transfer characteristic is linearized around a constant value, and then, the symmetrical optimum criterion is implemented to achieve controller gains.

**Control of the ST Inverter**

The ST inverter maintains balanced sinusoidal voltages at the LV ac line having a magnitude of 230 V rms per phase and frequency of 50 Hz. At all the time of operation, it supplies for load reactive and harmonic powers. Active power transfer depends upon the DG power availability. If the DG power is more than the load power demand, then the additional power is fed back to the LV dc link by the inverter. However, the power is extracted from the MV grid and/or BESS in case DG power is not sufficient to meet the load demands. The control of the LV stage is cascaded voltage–current control. The inner current control based on a proportional regulator allows damping the resonance of the LC filter, whereas the outer PI control is used for the voltage control [1].

**BESS SOC Control**

In the power flow analysis, it has been seen that the battery bank can have four operating conditions: charging mode, discharging mode, fully charged mode, and not fully charged mode. The BESS dc–dc converter remains operational in the first two modes, whereas in the last two modes, the converter remains in the standby mode. However, the converter must be able to switch between the different operational modes based on the control signal.

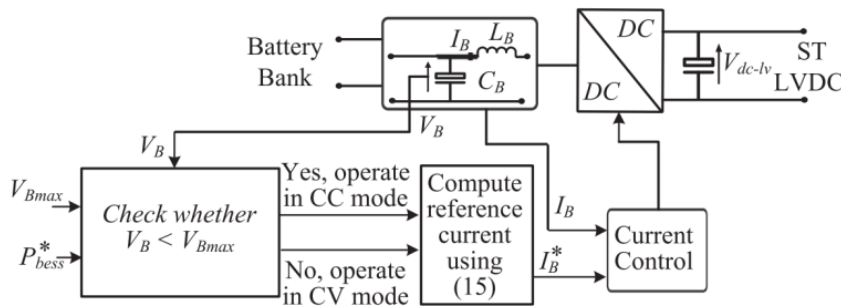


FIGURE 9. BESS control block diagram

The dc–dc converter of the BESS helps in maintaining the battery SOC within range during charging and allows us to support the loads during discharging. Let the power exchanges by the BESS be  $P_{bess}$  at any given time, and it can be given as follows:

$$P_{bess} = V_B I_B$$

where  $V_B$  and  $I_B$  are voltage across the battery bank and the current exchanged by the battery bank. As long as the voltage across the battery bank remains below the maximum value ( $V_{Bmax}$ ) during the charging, the BESS is operated in the constant current (CC) mode. Once the battery voltage reaches maximum set point values, the BESS is operated in the constant voltage (CV) mode [4]. Moreover, once the battery bank achieves the maximum SOC, the dc–dc converter is operated in floating charging mode to keep the battery bank fully charged. In this case, a small amount of current is taken to overcome the battery self-discharge. The control block diagram is shown in Fig. 10. The PI-based controller generates an angle  $\delta$ , which is used to maintain the power balance [34]. Depending upon the different scenarios of the system configuration, the reference BESS power can be computed as follows.

Case I: DG power is greater than the load power demand, and the battery is not fully charged (battery SOC is smaller than  $SOC_{max}$ ). In this case, the rest of the power is used to charge the BESS:

$$P_{bess}^* = P_{DG} - P_l$$

Case II: DG power is greater than the load power demand, and the battery is fully charged (battery SOC is equal to  $SOC_{max}$ ). In this case, the BESS will not exchange any power:

$$P_{bess}^* = 0$$

Case III: DG power is lower than the load power demand, and the power deficit is smaller than the ST rectifier power rating; then the BESS will not exchange any power:

$$P_{\text{bess}}^* = 0$$

Case IV: Once the rectifier power reaches its rated value, i.e.,  $P_{\text{rec}} = P_{\text{rec-rated}}$ , then the deficit of the power is supplied by the BESS. This situation arises during peak load periods or during grid faults:

$$P_{\text{bess}}^* = P_l - P_{\text{DG}} - P_{\text{rec-rated}}$$

## Controller Design with ANFIS and Mathematical Analysis for ST-BESS

The integration of an Adaptive Neuro-Fuzzy Inference System (ANFIS) into the controller of a Smart Transformer-based Battery Energy Storage System (ST-BESS) is a cutting-edge solution that enhances the system's performance. The use of ANFIS in the controller provides a mechanism for adaptive, intelligent control that can handle the non-linearities and uncertainties associated with the operation of a BESS and ST. This section details the ANFIS-based controller, its working principle, and the mathematical analysis used to model and evaluate the system's performance.

### Overview of ANFIS-based Controller

The Adaptive Neuro-Fuzzy Inference System (ANFIS) is a hybrid intelligent system that combines the advantages of both neural networks and fuzzy logic. It employs the fuzzy inference system (FIS) to model the relationship between inputs and outputs in a linguistic way, while the neural network component is responsible for learning and adjusting the parameters of the fuzzy rules based on input-output data. In the context of the ST-BESS, the ANFIS controller is primarily responsible for managing the State of Charge (SOC) of the battery, ensuring that the battery operates within optimal charging and discharging limits. The controller uses real-time information about the grid load, renewable energy generation, and battery SOC to adaptively manage the charging and discharging cycles of the battery. The controller continuously updates its rules based on incoming data and adjusts the system's operation to ensure energy efficiency and system reliability.

Key inputs to the ANFIS controller include:

- SOC (State of Charge) of the battery.
- Load Demand on the grid.
- Renewable Energy Generation (such as solar or wind generation).
- Voltage and Frequency conditions from the grid.

The outputs of the ANFIS controller determine the charging or discharging rate of the battery and the optimal operation of the Smart Transformer.

### Mathematical Model of the ST-BESS with ANFIS Control

To understand the impact of the ANFIS controller, it is important to develop a mathematical model of the ST-BESS system. The model includes key components such as the battery, the Smart Transformer, and the interaction with the grid.

#### Battery Model:

The battery can be modelled by a first-order dynamic equation that represents the charging and discharging behavior. The state of charge (SOC) of the battery, denoted as  $C(t)$ , evolves over time depending on the current  $I(t)$  flowing into or out of the battery. The battery model is given by:

$$\frac{dC(t)}{dt} = \frac{I(t)}{C_{\text{max}}}$$

Where:

- ❖  $C(t)$  is the state of charge of the battery at time  $t$ .
- ❖  $C_{\text{max}}$  is the maximum capacity of the battery.
- ❖  $I(t)$  is the current (positive during charging, negative during discharging).

The current  $I(t)$  is determined by the control action of the ANFIS controller, which adjusts the charging or discharging rate based on the input signals.

#### Smart Transformer (ST) Model:

The Smart Transformer can be modeled as a power electronic converter that adjusts the voltage and current in response to control signals. The output of the Smart Transformer, PST, is related to the voltage  $V(t)$  current  $I(t)$  and impedance  $Z$  as follows:

$$P_{ST} = V(t)I(t) \cos(\theta)$$

Where:

- ❖  $V(t)$  is the output voltage of the ST.
- ❖  $I(t)$  is the current output.
- ❖  $\theta$  is the phase angle between the voltage and current.

The Smart Transformer manages the power conversion and regulates the voltage supplied to or from the battery, adapting to changing grid conditions.

#### Control Input and Output of ANFIS:

The control input to the ANFIS controller consists of the SOC of the battery, the load demand, and the renewable energy generation (solar/wind). The output of the ANFIS controller determines the charging and discharging rates of the battery. Let the inputs to the ANFIS system be:

- $x_1(t) = \text{SOC}(t)$
- $x_2(t) = \text{Load Demand}(t)$
- $x_3(t) = \text{Renewable Generation}(t)$

The output of the ANFIS controller,  $u(t)$ , represents the current  $I(t)$  to be supplied to the battery:

$$u(t) = f(x_1(t), x_2(t), x_3(t))$$

Where  $f$  is the fuzzy inference function learned by the ANFIS. The fuzzy inference system (FIS) can be defined using fuzzy membership functions. Typically, these functions might be triangular or Gaussian functions. Based on the inputs, fuzzy rules are generated to decide the battery charging/discharging strategy. For example, if the SOC is low, the load demand is high, and renewable energy generation is insufficient, the ANFIS might output a high discharging rate to meet the demand. Conversely, if the SOC is high and renewable energy is abundant, the controller may choose a charging action.

#### ANFIS Controller Design and Mathematical Analysis

The ANFIS controller design involves the following steps:

##### Fuzzification:

The input variables (SOC, load demand, renewable generation) are fuzzified using membership functions. For instance:

$\mu_{\text{SOC}}(x_1)$  = membership function for SOC

$\mu_{\text{Load}}(x_2)$  = membership function for load demand

$\mu_{\text{Renewable}}(x_3)$  = membership function for renewable generation

##### Rule Base Generation:

Fuzzy rules are defined based on expert knowledge or empirical data. A simple example of a rule base could be:

- IF SOC is LOW AND Load is HIGH AND Renewable Generation is LOW THEN Discharge Rate is HIGH.
- IF SOC is HIGH AND Load is LOW AND Renewable Generation is HIGH THEN Charge Rate is HIGH.

##### Inference Mechanism:

The fuzzy inference process involves applying the fuzzy rules to the inputs. The system evaluates each rule's output using a fuzzy implication (e.g., Mamdani or Takagi-Sugeno inference method).

##### Defuzzification:

The final crisp output (charging or discharging current  $I(t)$ ) is obtained by defuzzifying the results of the inference process. The most common defuzzification method is the centroid method:

$$u(t) = \frac{\sum_i w_i \cdot c_i}{\sum_i w_i}$$

Where:

- $w_i$  is the weight of each rule.

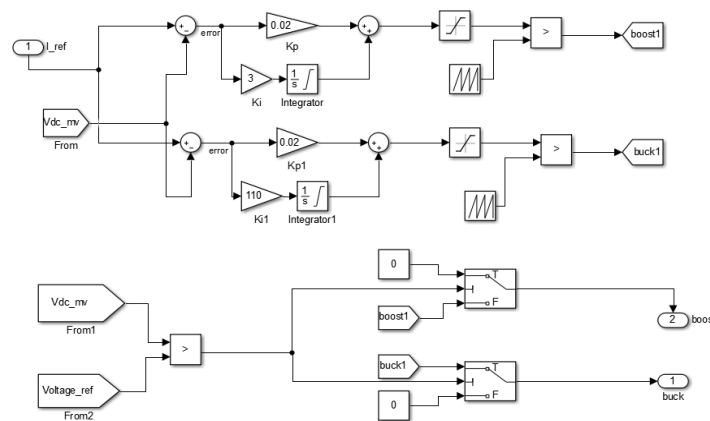
- $ic\_ici$  is the output of each rule.

### Learning and Optimization:

The parameters of the membership functions are adjusted during the learning process using a neural network. The error is computed between the predicted and actual output values, and the parameters are updated using backpropagation or gradient descent methods. The integration of an ANFIS-based controller into the Smart Transformer-based Battery Energy Storage System (ST-BESS) brings significant improvements in terms of system performance, adaptability, and energy efficiency. The ANFIS controller enables intelligent decision-making based on real-time system data, optimizing the charging and discharging cycles of the battery while maintaining grid stability. The mathematical analysis of the system, including the battery model, ST power conversion, and control algorithms, provides a detailed understanding of the system dynamics and enables the design of optimal control strategies. Through both simulation and experimental validation, the effectiveness of the ANFIS controller in enhancing the performance of the ST-BESS can be confirmed, making it a powerful solution for modern grid management and renewable energy integration.

## 4. SIMULATION RESULTS

The simulations are carried out in PSCAD software to show the performance of the proposed configuration during few operating conditions. It is considered that the battery bank is charged enough to support the loads. The first case is shown in Fig. 11. The MV grid voltage, ST rectifier currents, LV ac voltages, LV-side ST currents, and different active powers are shown in Fig. 11(a)–(e), respectively. The steady-state condition is shown from  $t = 1$  to 2 s, where the load power demand is greater than DG power. In this case, the power deficit is supplied by the MV grid for maintaining power balancing. At  $t = 2$  s, a voltage dip of 40% is created in the MV grid. If we consider the conventional BESS-based system, the overall BESS and the loads must be disconnected from the MV grid, while operating the overall system in the islanded mode. This operation again requires to be synchronized with the grid. Moreover, in the proposed configuration the system remains connected to the MV grid. The ST rectifier draws active power from the MV grid, depending upon the available rms current of the device. Once the rated current for the ST rectifier is reached, the remaining load power requirement is supplied by the BESS. It can be seen from figure that during the voltage dip, the ST current reaches its rated value to draw appropriate power. The BESS gets activated to support the rest load power requirement. Moreover, the DG power remains constant. Moreover, once the voltage is restored at  $t = 3$  s, the BESS power becomes zero, and the normal operation is restored. This feature of the proposed scheme allows the system to remain connected to the grid during voltage dips, which cannot be achieved in the conventional scheme. The second case, as shown in Fig. 12, provides the system performance during the peak load condition. It can be seen that the load power is 500 kW from  $t = 1$  to 3 s, which is shared by the DG power and the MV grid. Moreover at  $t = 3$  s, the load power changes to 675 kW. This power cannot be taken from the MV grid as the ST rectifier active power is limited to 575 kW. In this case, the ST rectifier currents increase to draw its rated power from the MV grid. The remaining power required by the load is supplied by the BESS. These waveforms are shown in Fig. 12. Moreover, once the loads are reduced at  $t = 5$  s to the normal value, the control scheme detects that the load requirement can be met by the DG and the MV grid using ST power converters, and hence, the BESS power output slowly becomes zero.

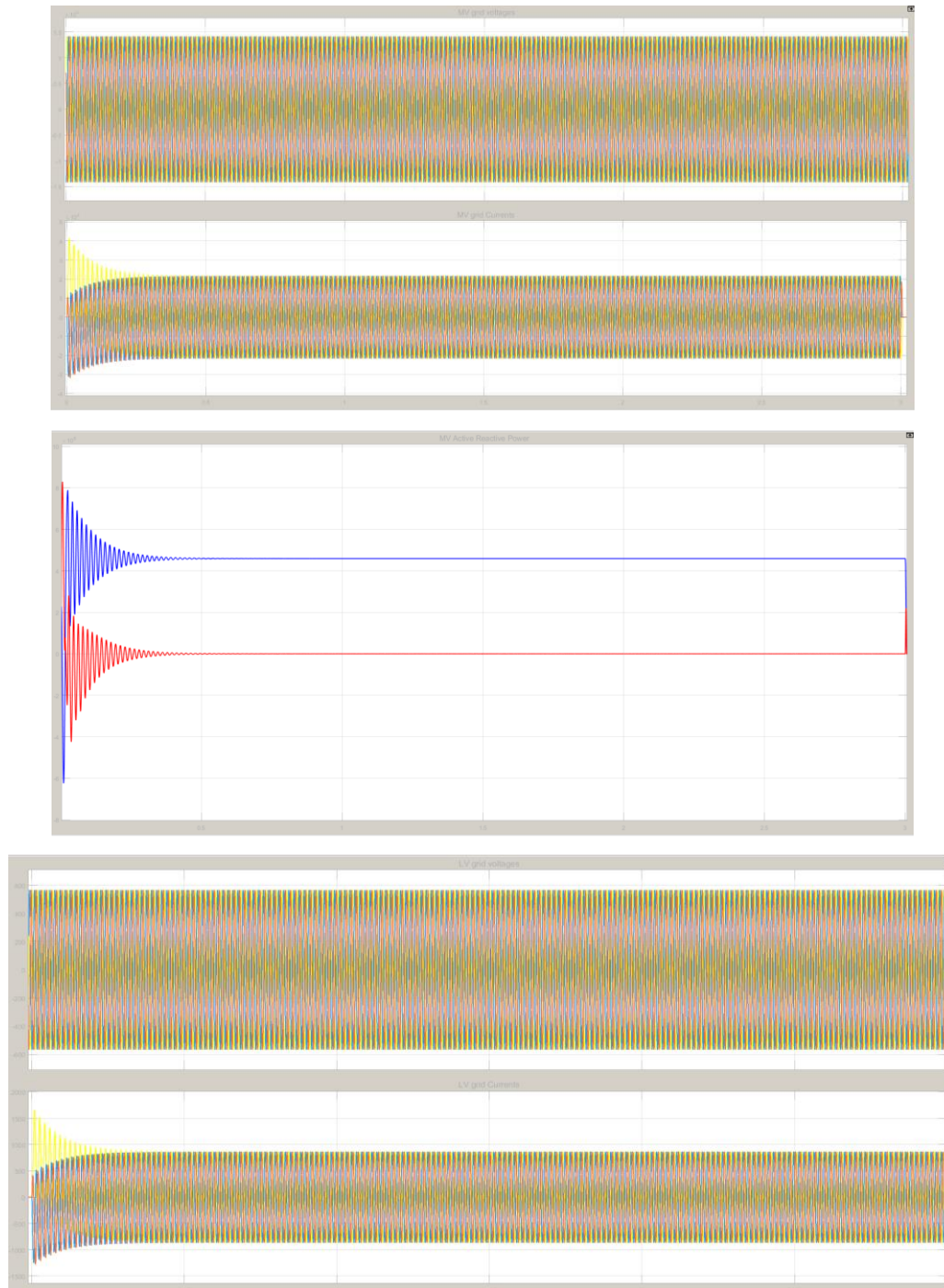


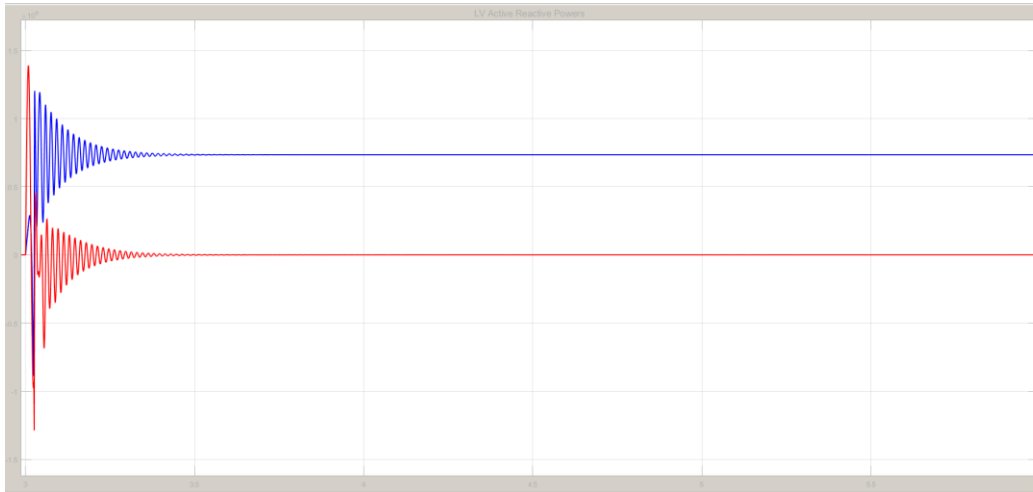
CURRENT CONTROLLER DC/DC BIDIRECTIONAL CONVERTER

FIGURE 10

The simulations are carried out in PSCAD software to show the performance of the proposed configuration during few operating conditions. It is considered that the battery bank is charged enough to support the loads. The MV grid voltage, ST rectifier currents, LV ac voltages, LV-side ST currents, and different active powers. The steady-state condition is shown from  $t = 1$  to 2 s, where the load power demand is greater than DG power. In this case, the power deficit is supplied by the MV grid for maintaining power balancing. At  $t = 2$  s, a voltage dip of 40% is created in the MV grid. If we consider

the conventional BESS-based system, the overall BESS and the loads must be disconnected from the MV grid, while operating the overall system in the islanded mode. This operation again requires to be synchronized with the grid. Moreover, in the proposed configuration, the system remains connected to the MV grid. The ST rectifier draws active power from the MV grid, depending upon the available rms current of the device. Once the rated current for the ST rectifier is reached, the remaining load power requirement is supplied by the BESS. It can be seen from figure that during the voltage dip, the ST current reaches its rated value to draw appropriate power. The BESS gets activated to support the rest load power requirement. Moreover, the DG power remains constant. Moreover, once the voltage is restored at  $t = 3$  s, the BESS power becomes zero, and the normal operation is restored. This feature of the proposed scheme allows the system to remain connected





**FIGURE 11.** Simulation results of the proposed configuration during voltage sag. (a) MV grid voltages. (b) ST rectifier current. (c) LV-side ST voltages. (d) LV-side ST currents. (e) Different active powers (normal operation for time interval T1 and T3 and operation during voltage sag for interval T2 )



**FIGURE 12.** Moreover, once the loads are reduced to the normal value, the control scheme detects that the load requirement can be met by the DG and the MV grid using ST power converters, and hence, the BESS power output is stable

## 5. CONCLUSION

This paper presented an investigation into the performance of a Smart Transformer (ST)-based Battery Energy Storage System (BESS) and compared it with conventional BESS in terms of energy efficiency during charging and discharging processes. The results demonstrated that the ST-based BESS outperforms the conventional system, particularly with regard to energy efficiency. Additionally, by appropriately sizing the BESS to meet peak load demands, the power rating of the ST converters can be minimized, making the system more cost-effective. The ST-based BESS also showed significant improvements in fault ride-through capabilities compared to traditional systems, enhancing grid stability and reliability. A key aspect of the ST-based BESS operation is effective state of charge (SOC) management, particularly when the ST converter operates at its maximum active power rating. To address this, an Adaptive Neuro-Fuzzy Inference System (ANFIS) was implemented for optimal SOC management, ensuring that the system could efficiently meet peak load demands while preventing over-discharge or over-charge conditions. Both simulation and experimental results validated the ANFIS-based SOC management approach, confirming its effectiveness in enhancing the overall system performance and reliability.

## 6. FUTURE SCOPE

Future research can focus on further improving the performance of the ST-based BESS by exploring advanced control algorithms for even more efficient SOC management, especially under dynamic load and grid conditions. The integration of machine learning techniques and predictive analytics could enable real-time optimization, improving both energy efficiency and operational stability. Additionally, expanding the ST-based BESS to support higher capacities or multi-unit configurations could make it suitable for large-scale applications, such as in industrial or utility-scale energy storage

systems. Exploring the potential for integrating renewable energy sources, such as solar or wind, with the ST-based BESS could further enhance the system's versatility and contribution to sustainable energy solutions. Further investigation into the fault tolerance and robustness of the ST converter, particularly under extreme operating conditions or faults, could lead to improved fault detection and mitigation strategies, enhancing the system's reliability. Finally, a comprehensive cost-benefit analysis and life-cycle assessment would be valuable for evaluating the long-term economic feasibility of deploying ST-based BESS in various grid applications, ensuring that the technology can meet the growing demands for efficient and reliable energy storage.

## REFERENCES

- [1]. R. Teodorescu, M. Liserre, and P. Rodriguez, *Grid Converters for Photovoltaic and Wind Power Systems*, vol. 29. New York, NY, USA: Wiley, 2011.
- [2]. H. Rahimi-Eichi, U. Ojha, F. Baronti, and M. Y. Chow, "Battery management system: An overview of its application in the smart grid and electric vehicles," *IEEE Ind. Electron. Mag.*, vol. 7, no. 2, pp. 4–16, Jun. 2013.
- [3]. C. S. Lai and M. D. McCulloch, "Sizing of stand-alone solar PV and storage system with anaerobic digestion biogas power plants," *IEEE Trans. Ind. Electron.*, vol. 64, no. 3, pp. 2112–2121, Mar. 2017.
- [4]. T. V. Thang, A. Ahmed, C. i. Kim, and J. H. Park, "Flexible system architecture of stand-alone PV power generation with energy storage device," *IEEE Trans. Power Convers.*, vol. 30, no. 4, pp. 1386–1396, Dec. 2015.
- [5]. J. von Appen, T. Stetz, M. Braun, and A. Schmiegel, "Local voltage control strategies for PV storage systems in distribution grids," *IEEE Trans. Smart Grid*, vol. 5, no. 2, pp. 1002–1009, Mar. 2014.
- [6]. K. Y. Lo, Y. M. Chen, and Y. R. Chang, "Bidirectional single-stage gridconnected inverter for a battery energy storage system," *IEEE Trans. Ind. Electron.*, vol. 64, no. 6, pp. 4581–4590, Jun. 2017.
- [7]. M. Liserre, G. Buticchi, M. Andresen, G. D. Carne, L. F. Costa, and Z. X. Zou, "The smart transformer: Impact on the electric grid and technology challenges," *IEEE Ind. Electron. Mag.*, vol. 10, no. 2, pp. 46–58, Jun. 2016.
- [8]. S. Bhattacharya, "Transforming the transformer," *IEEE Spectr.*, vol. 54, no. 7, pp. 38–43, Jul. 2017.
- [9]. X. She, A. Q. Huang, and R. Burgos, "Review of solid-state transformer technologies and their application in power distribution systems," *IEEE Trans. Emerg. Sel. Topics Power Electron.*, vol. 1, no. 3, pp. 186–198, Sep. 2013.
- [10]. M. Andresen, K. Ma, G. D. Carne, G. Buticchi, F. Blaabjerg, and M. Liserre, "Thermal stress analysis of medium-voltage converters for smart transformers," *IEEE Trans. Power Electron.*, vol. 32, no. 6, pp. 4753–4765, Jun. 2017.